Measuring Adhesion Strength of Wall Tile to Concrete by Non-Contact Inspection Using Electromagnetic Waves

Hussain Alsalem [a], Takayuki Tanaka[b], Takumi Honda[c], Satoru Doi [d], Shigeru Uchida[e]
[a]Department of Information Science, University of Hokkaido, Japan
[b]Department of Information Science, University of Hokkaido, Japan
[c]Central Research Institute of Electric Power Industry, 2-6-1, Kanagawa, Japan
[d]Obayashi Corporation, Tokyo, Japan
E-mail: hussain@hce.ist.hokudai.ac.jp, ttanaka@ssi.ist.hokudai.ac.jp, honda3793@criepi.denken.or.jp, {doi.satoru, uchida.shigeru }@obayashi.co.jp

Abstract **–** The separation of exterior tiles from buildings diminishes the visual appeal of cities and can injure pedestrians when they are struck by falling tiles. Therefore, tiles should be inspected periodically. However, completion of the inspection process has hurdles, including high cost and the need for qualified human inspectors. This study describes a non-destructive inspection method for detecting voids that match those seen in tile separation in a concrete specimen using electromagnetic waves, specifically microwaves. The method can be performed using devices that are simpler, smaller, and easier to use than those required by conventional methods. In addition, this method can be used to measure the adhesion strength of tiles.

Keywords **– Non-contact inspection; Electromagnetic wave; Adhesion strength; Multi-layered scanning.**

1 Introduction

The separation of exterior tiles from buildings reduces the visual attractiveness of cities and falling tiles can injure pedestrians below, especially during earthquakes. Therefore, tiles should be checked periodically. However, high cost and the need for a qualified human inspector hinders the completion of inspections. In this study, voids that match those seen in tile separation were detected in a tiled concrete specimen using non-destructive inspection (NDI) with electromagnetic waves (EMWs), specifically microwaves. Several methods based on NDI techniques using EMWs have been developed and reported. These methods include ground-penetrating radar [1], microwave tomography [2], microwave non-destructive testing, and other evaluation methods [3] [4] that use a network analyser in the time/frequency domain to calculate the position of foreign bodies in the object; such methods are very complex and costly.

Our proposed method uses EMW reflection intensity data for analysis, and the measuring device required is simpler, smaller, and easier to use than that required for the above-mentioned methods. Our method can also use the reflection data to estimate the adhesion strength of the tiles. An antenna that transmits and receives microwaves was used to obtain the reflection intensity from the concrete specimen, and the distribution of reflection intensity was determined using a multi-layered scanning (MLS) method. This reflection intensity was compared with normal concrete data (trend data) to predict the integral of the difference, which indicates the size of the void [5] [6]. In our experiments, first, a tiled concrete specimen with voids was evaluated by MLS to calculate the strength distribution. Second, tensile strength testing of the tiled concrete was performed, and the strength to failure was measured. Third, the correlation between the tensile strength and the reflection intensity by MLS was examined to evaluate the possibility for practical use.

2 Microwave NDI

2.1 Inspection apparatus

The inspection apparatus for detecting voids consists of a linear actuator and a flaw detection device. The flaw

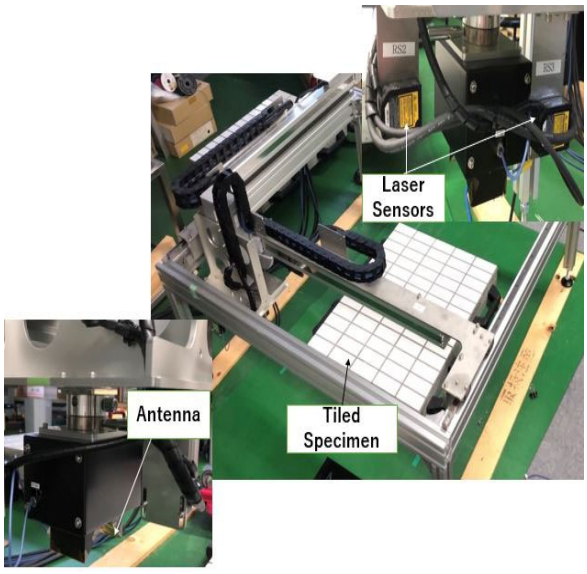

Figure 1. Inspection apparatus.

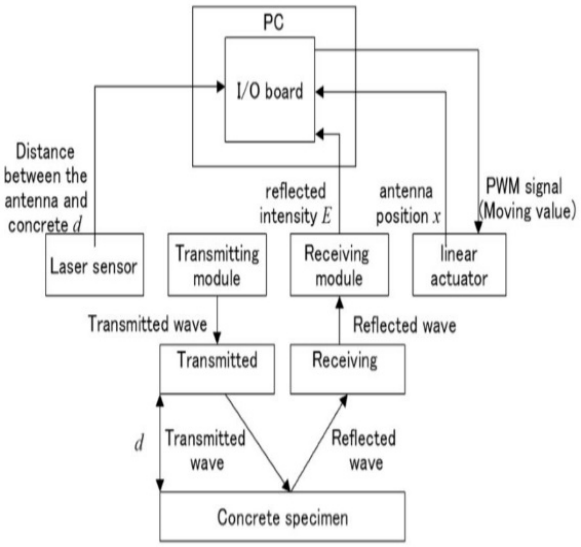

Figure 2. Measurement system.

detection device consists of a lifter, an antenna, and a laser sensor, as shown in Figure 1. An overview of the signal processing system is shown in Figure 2. The linear actuator is used to move the flaw detection device over the concrete surface, and the device scans the surface to detect voids.

2.2 Tiled concrete specimen

Figure 3 shows the tiled concrete specimen, which comprises tiles, adhesive mortar, and concrete. Figure 4(a) shows the dimensions of the tiled concrete and the positions and widths of the voids, Figure 4(b) shows the design of the tiled concrete specimen from the side, and Figure 4(c) shows the positions of the voids as seen from the side. The experiments demonstrate the effectiveness of the proposed void detection method by applying NDI using EMWs to an actual tiled concrete specimen. In addition, the system used the void sizes to indicate the tile adhesion strength.

2.3 MLS method

This section describes the MLS method [5-6], which is used to acquire the reflected intensity and to estimate and remove interference and noise caused by EMWs.

The detection void algorithm is shown in Figure 5. First, the total reflection intensity, E_r, is measured by MLS. In abnormal areas, the received intensity is the effective value of the sum of the direct wave, surface wave, and air gap reflected wave. Next, the trend reflection intensity, E_t, is measured by MLS. This shows the reception intensity of normal (void less) areas, which is the effective value of the sum of the direct wave and

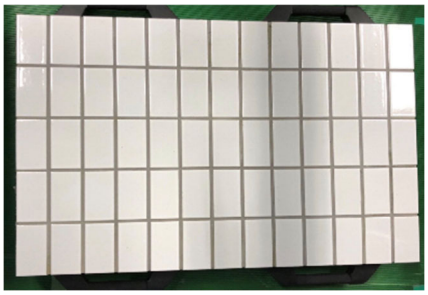

Figure 3. Tiled concrete specimen.

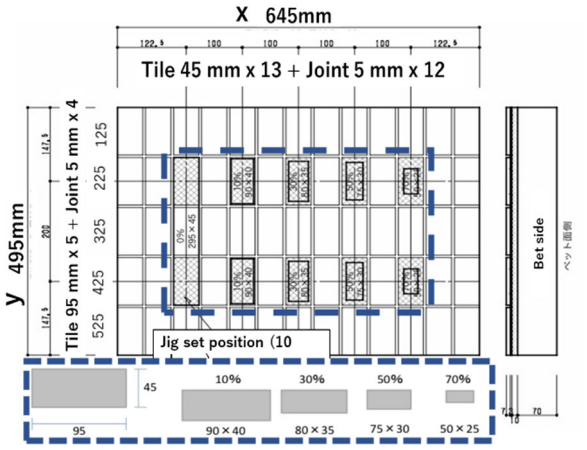

(a) Concrete dimensions and void positions and widths.

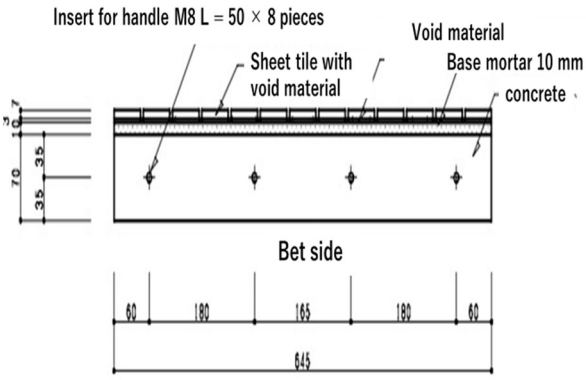

(b) Side view of concrete specimen design.

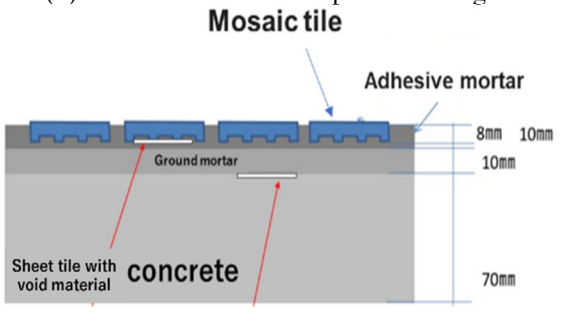

(c) Side view of void positions

Figure 4. Experimental setup.

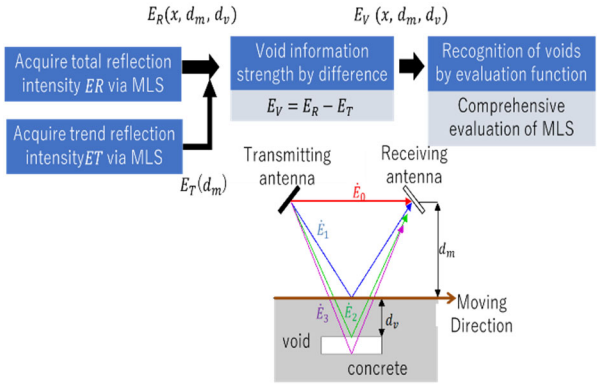

Figure 5. Algorithm for void detection.

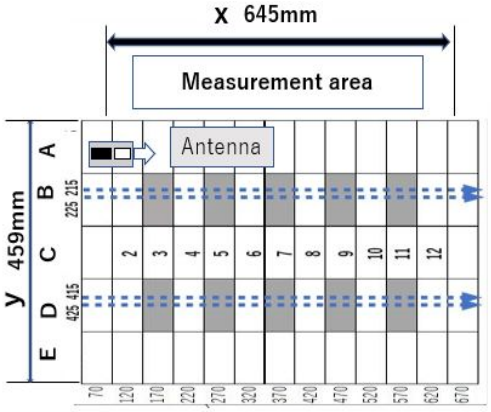

Figure 6. Overview of tiled specimen scanning.

the surface wave. Then, void reflection intensity E_v is obtained by taking the difference between the total reflection intensity and the trend intensity strength. The last step recognizes voids by a comprehensive evaluation of MLS.

2.3.1 Detecting voids

This section shows how an evaluation function $P(x)$ can quantitatively detect voids from the measured reflected intensity. $P(x)$ can detect voids from $\hat{E}_v(x, d)$ which is the void information is obtained by taking the difference between $E_t(d)$ and $E_t(x, d)$. This compensation makes the scanning more robust against the noise caused by small variations in d. Hence, this procedure should be useful for scanning a real tiled wall. And is defined as

$$P(x) = \frac{1}{N}\sum_i^n |\hat{E}_v(x, d_i)| \quad (1)$$

where N is the number of data points along the d-axis at each value of x. Because $\hat{E}_v(x, d)$ is obtained from the difference between reflected intensities, it can be negative. By removing the variation of d, scanning collects only the reflected intensity from the voids and the concrete, allowing the voids to be detected and distinguished more easily.

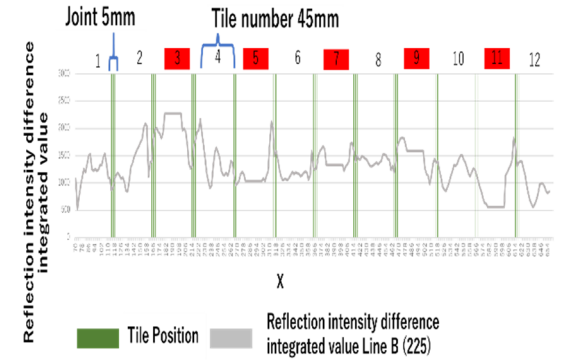

(a) $y = 215$ mm (Line B 225).

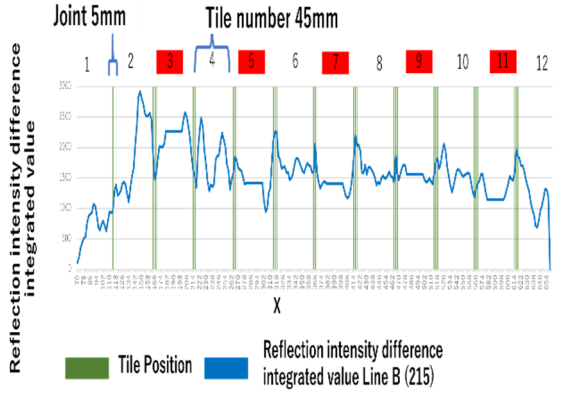

(b) $y = 225$ mm (Line B 215).

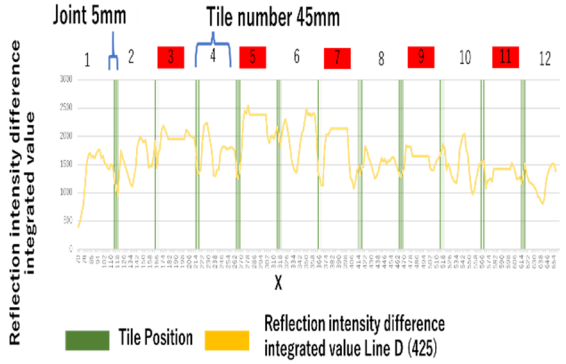

(c) $y = 415$ mm (Line D 425).

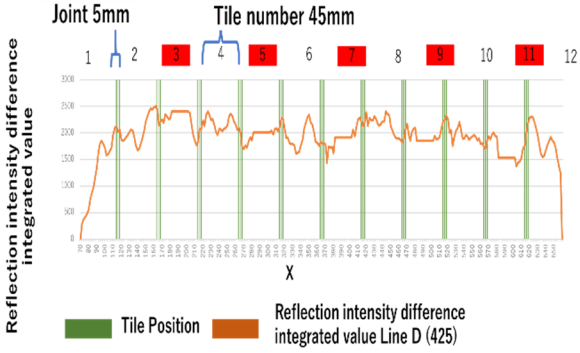

(d) $y = 425$ mm (Line D 415).

Figure. 7. Distribution of $P(x)$ at various tile locations.

2.3.2 MLS measurement results

Experiments were conducted using real tiled concrete to demonstrate the effectiveness of the proposed method for inspecting actual tiled walls. The concrete specimen shown in Figure 3 comprises the tile, its adhesive mortar, and concrete. MLS was performed at $y = 215, 225, 415, \text{and } 425$ mm, with a measurement area as shown in Figure 6. Intensity $E_R(x, d)$ was obtained by scanning along the x-axis in each scanning area several times at intervals of $60 \text{ mm} < d < 90 \text{ mm}$. through changing y-axis, we can set up the Anita in position of Line. The evaluation function $P(x)$ using this result is shown in Figure 7. The vertical axis shows the variation of the integrated reflection intensity, which varies according to whether voids are present. The average integrated reflection intensity was taken at a distance ± 10 mm from joints. The horizontal axis is the tile position. Red tiles have voids ranging from 30% to 100% of the tile size. Other tiles are normal tiles without voids. In most scanning lines, the integrated reflection intensity is high at large voids and low at small voids.

Figure 8. Manual Pull-off adhesion tester.

Figure 9. Tile removal operation. Nuts are installed on the tiles to be removed.

3 Tile pulling test

3.1 Inspection Apparatus

Measurement of the adhesion strength was demonstrated using a pull-off adhesion tester (LPT-3000, Ox Jack Co., Ltd.). Before using the adhesion tester, a hammering test was performed to determine whether a void was present. Figure 8 shows the tester, which

Table 1. Adhesion test results

Tile position	Void size (%)	Load (kN)	Load (N/mm^2)	Integrated reflection intensity V
Line D 425, No. 3	100	0.2	0.047	$1{,}995 \le V \le 2{,}091$
Line D 415, No. 3	100	0.2	0.047	$2{,}213 \le V \le 2{,}748$
Line B 225, No. 3	100	0.2	0.047	$2{,}072 \le V \le 2{,}542$
Line B 215, No. 3	100	0.2	0.047	$1{,}962 \le V \le 2{,}526$
Line D 425, No. 5	90	0.2	0.047	$1{,}883 \le V \le 2{,}011$
Line D 415, No. 5	90	0.2	0.047	$2{,}213 \le V \le 2{,}748$
Line B 225, No. 5	90	0.5	0.12	$978 \le V \le 1{,}255$
Line B 215, No. 5	90	0.5	0.12	$1{,}962 \le V \le 2{,}526$
Line D 425, No. 7	70	1.8	0.42	$1{,}080 \le V \le 1{,}262$
Line D 415, No. 7	70	1.8	0.42	$1{,}611 \le V \le 2{,}260$
Line B 225, No. 7	70	2.5	0.58	$1{,}155 \le V \le 1{,}364$
Line B 215, No. 7	70	2.5	0.58	$1{,}310 \le V \le 1{,}448$
Line D 425, No. 9	50	2.3	0.54	$1{,}403 \le V \le 1{,}577$
Line D 415, No. 9	50	2.3	0.54	$1{,}727 \le V \le 2{,}026$
Line B 225, No. 9	50	1.5	0.35	$1{,}532 \le V \le 1{,}744$
Line B 215, No. 9	50	1.5	0.35	$1{,}402 \le V \le 1{,}674$
Line D 425, No. 11	30	1.8	0.42	$1{,}244 \le V \le 1{,}533$
Line D 415, No. 11	30	1.8	0.42	$1{,}403 \le V \le 1{,}755$
Line B 225, No. 11	30	4.5	1.05	$379 \le V \le 739$
Line B 215, No. 11	30	4.5	1.05	$964 \le V \le 1{,}316$

consists of an analogue load cell, a pump handle, and an attachment. When the pump handle is turned clockwise, the attachment rises and pulls the tile until it separates from the concrete, as shown in Figure 9. At the moment of tile removal, the strength is measured by the load cell and recorded. The recorded load data are shown in Table 1, columns 3 and 4.

3.2 Results of adhesive strength measurements and MLS analysis

Figure 10(a) and (b) show the values of exact value of P(x) of all lines at locations of each tile for which adhesion strength was tested. The six points of P(x) was taken over a total distance of 20 mm and ± 10 mm from joints to avoid effects from the joints themselves [6]. The points were distributed on Lines B 215, B 225, D 415, and D 425. Data recorded from the tile pulling tests and MLS analysis are shown in Table 1. Column 1 shows the location of each tile for which adhesion strength was tested and MLS was performed. Column 2 is the void size, which varied from 30% to 100% of the tile size in 20% increments. Column 3 shows the recorded pull strength data in kilonewtons, which is the power required to remove the tile and is directly analogous to load cell results. In column 4, the power is converted to newtons per square millimetre. MLS results are shown in column 5. Based on the adhesive strength and MLS data from Figure 10(a) and (b), Table 1, the scatter plot in Figure 11 was created. This plot shows the adhesive strength of all lines on the horizontal axis and integrated reflection intensity on the vertical axis. The intersection of the two values is shown by colours indicating the tile and scanning position.

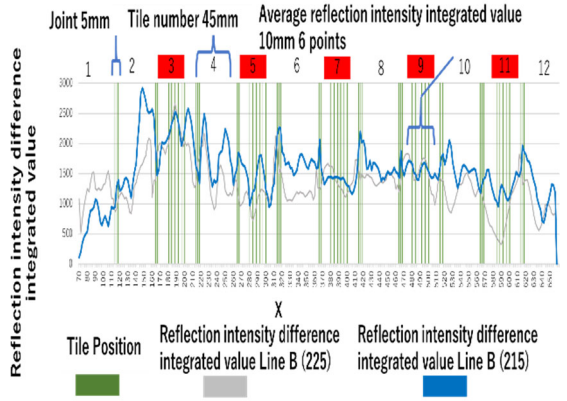

(a) $y = 225$ mm (Line B 225) and$y = 215$ mm (Line B 215).

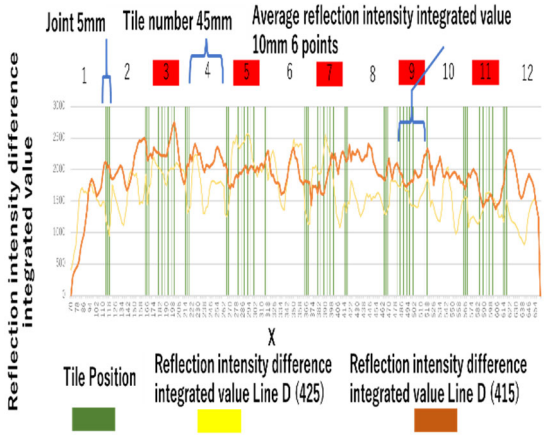

(b) $y = 425$ mm (Line D 425) and$y = 415$ mm (Line D 215).

Figure 10. Distribution of tensile bond strength.

3.3 Analysis of adhesive strength measurements and MLS results

The results of adhesive strength measurements plotted against MLS values in Figure 11 indicate that there is a negative correlation between adhesive strength and the value of the tensile strength. Also, there appears to be a linear relationship between the two variables. Testing of the significance of the correlation coefficient confirmed a strong negative correlation, meaning that a decreased tensile bond strength is correlated with increased integrated reflection intensity, with $R = -0.622$ at $p < 0.001$. Furthermore, regression analysis provided the result $R^2 = 0.382$ at $p < 0.001$.

3.4 Discussion

The results show that this method can estimate the adhesion strength, but with a large error. The regression analysis R-squared result is significantly low. This low value might be caused by the experimental procedure, or it might indicate that there was a problem in how voids were implanted under the tile to make the specimen. As

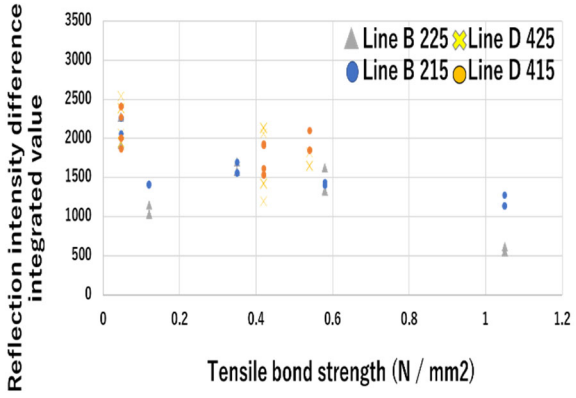

Figure 11. Reflection intensity integrated value versus tensile bond strength

seen in Figure 10(a), in Line D 425, tile No. 3 has a void size bigger than that of No. 5. Therefore, it should have a higher intensity value. However, the integrated value for reflection intensity difference is lower. In Line B, tile Nos. 7 and 8 have the same issue. These issues might have occurred because the tiled concrete specimen was not cured. Environmental effects on sheet strength due to the time that elapsed between performing MLS and measuring the tensile strength needs to be taken into consideration. To improve the accuracy of the estimation, more data are needed by analysing tiles of different sizes. In addition, the experimental procedure would be improved if the MLS scanning data and the adhesive strength were obtained at the same time. Furthermore, a more accurate adhesive strength measurement device should be used.

4 Concluding Remarks

This paper describes ability of the MLS method in determining tile adhesive strength. This method will increase the accuracy of the safety tests required for wall tiles used in building exterior finishes. In particular, the MLS method does not require an expert to implement it. Therefore, it has the potential to reduce the cost and time required for tile safety examinations.

References

[1] Xu. X, Xia. T, Venkatachalam. A, and Huston. D, "Development of high-speed ultrawideband ground-penetrating radar for rebar detection," Journal of Engineering Mechanics, Vol.139, No.3, pp.272-285, 2012.

[2] Kim. Y. J. Jofre. L, De Flaviis. F, and Feng. M. Q, "Microwave reflection tomographic array for damage detection of civil structures," IEEE Transactions on Antennas and Propagation, Vol.51, No.11, pp.3022-3032, 2003.

[3] Arunachalam. K, Melapudi. V. R, Udpa. L, and Udpa. S. S, "Microwave NDT of cement-based materials using far-field reflection coefficients," NDT and E International, Vol.39, No.7, pp.585-593, 2006

[4] Zoughi. R, and Bakhtiari. S, "Microwave nondestructive detection and evaluation of voids in layered dielectric slabs," Research in Nondestructive Evaluation, Vol.2, No.4, pp.195-205,1990.

[5] Kawataki. S, Tanaka. T, Doi. S, Uchida. S, and Feng. M. Q, "Nondestructive In-spection of Voids in Concrete by Multi-layered Scanning Method with Electro-magnetic Waves," Proc. of the IEEE International Conference on MECHA-TRONICS (IEEE-ICM2017), pp. 336-341,2017.

[6] T. Honda, T. Tanaka, S. Doi, S. Uchida, and M. Feng, “Visualization of Voids Between Tile and Concrete by Multi-Layered Scanning Method with Electromagnetic Waves,” J. Robot. Mechatron., Vol.31, No.6(2019) 863-870